1 **Drought Legacies Mediated by Trait Tradeoffs in Soil Microbiomes**

2

3 Bin Wang [1], Steven D. Allison [1,2]

4 [1] Department of Ecology and Evolutionary Biology, University of California, Irvine, CA

5 [2] Department of Earth System Science, University of California, Irvine, CA

6   **Abstract:** Soil microbiomes play a key role in driving biogeochemical cycles of the Earth system.

7   As drought frequency and intensity increase due to climate change, soil microbes and the processes

8   they control will be impacted. Even after a drought ends, microbiomes and other systems take time

9   to recover and may display a "memory" of previous climate conditions. Still, the mechanisms

10   involved in these legacy effects remain unclear, making it difficult to predict climate and

11   biogeochemical rates in the future. Here, we used a trait-based microbiome model to analyze

12   mechanisms underlying drought legacy effects on litter decomposition. We represented cellular

13   tradeoffs between osmolytes required for drought tolerance and investment in enzymes involved

14   in litter decomposition. Simulations were run under varying levels of drought severity and

15   dispersal. When dispersal was restricted, we found persistent drought legacies following severe

16   drought and transient legacies following moderate drought. With dispersal, there were no legacy

17   effects on litter decomposition. Greater movement along the tradeoff between enzyme investment

18   and osmolyte production resulted in stronger legacy effects. We organized these legacy outcomes

19   according to the YAS framework defined by tradeoffs between Y (Yield), A (Acquisition), and S

20   (Stress tolerance), three primary life history strategies of microorganisms. Factors that change the

21   trajectory of a community in YAS space may alter the legacy outcome following drought. This

22   trait-based mechanistic insight into drought legacies offers promise for more accurately predicting

23   soil microbiome resilience and functioning. Our study illustrates an emerging approach for

24   representing trait tradeoffs in microbiomes and vegetation that dictate ecosystem responses to

25   drought and other environmental perturbations.

26

1 Introduction

Drought of increasing severity and frequency both regionally and worldwide is an important environmental change affecting the Earth system (e.g., **Borsa et al. 2014; Berdugo et al. 2020**). The soil microbiome is a key driver of element cycling (e.g., **Falkowski et al. 2008**), so microbial responses are integral for evaluating drought impacts on ecosystem biogeochemistry. Still, these responses are omitted or implicitly treated in global assessments of drought-biosphere interactions (e.g., **Green et al. 2019**).

Over a half-century of research has uncovered myriad physico-chemical, physiological, and ecological mechanisms underlying microbial functional responses to drought disturbance in soil environments (e.g., **Birch 1958; Schimel 2007; Manzoni et al. 2012**). Moreover, multiple studies have suggested that drought may have lasting effects on the soil microbiome and its functioning, even after drought conditions have ended (e.g., **Evans and Wallenstein 2012**; **Meisner et al. 2015**; **Hawkes et al. 2017; Martiny et al. 2017; Hinojosa et al. 2019**). This phenomenon, here termed drought legacy, has also been observed in forests and other biomes (e.g., **Cuddington 2011; Anderegg et al. 2015; Conradi et al. 2020**). Still, the mechanistic basis for microbial drought legacies remains unclear. Such a lack of mechanistic information hinders the ability to predict drought impacts on ecosystem processes.

Legacies likely originate from microbiome changes that persist after a drought disturbance. Microbiomes are complex adaptive systems, with their functioning emerging from both individual variation and within-community interactions. Also, plant responses to drought may also impact this functional emergence and contribute to legacy effects (e.g., **Kaisermann et al. 2017**). Past lab- and field-based studies explained soil microbial drought legacies by framing compositional differences in terms of microbial functional groups with different life-history strategies. Notably,

3

50 **Hawkes and Keitt (2015)** proposed a mechanism driven by shifts in relative abundance of

51 moisture generalists vs. specialists, where generalists are functionally more stable than specialists

52 with variations in moisture. Along a rainfall gradient in Texas, USA, high variability in historical

53 rainfall was thought to select for dominance by generalist taxa, resulting consistency in moisture

54 responses across sites (**Hawkes et al. 2017; Waring and Hawkes 2018**). Similarly, **Evans and**

55 **Wallenstein** (**2014**) argued that soils with relatively stable moisture history had more moisture-

56 sensitive taxa and hence larger changes in biomass and composition following drought (**Evans**

57 **and Wallenstein 2012**).

58 Functional groupings are based on physiological traits and can help simplify complex

59 microbiomes but may obscure important physiological and ecological details. For instance,

60 microbial cells can re-direct resource allocation from exoenzyme production to osmolytes that

61 confer desiccation resistance (e.g., **Schimel 2007**), an intra-cellular metabolic strategy that

62 displays large inter-cellular variability (e.g., **Manzoni et al. 2012**). Without representing these

63 physiological processes, models may have difficulty predicting microbial community responses to

64 drought disturbance and the consequences for functioning. Addressing this challenge could help

65 reconcile studies that report drought legacies of varying magnitudes with differing time frames,

66 including those that observed no legacy (e.g., **Rousk et al. 2013; Fuchslueger et al. 2016**). A

67 similar lack of mechanistic understanding also applies to warming-induced legacies in microbiome

68 functioning (e.g., **Karhu et al. 2014**). Linking individual-level physiological variation to

69 community-level shifts could help fill this gap in knowledge of microbial functioning with

70 environmental change.

71 Trait-based approaches for dealing with ecological complexity can bridge the gap between

72 community dynamics and physiological variation that may underpin drought legacies in

73   microbiomes. Such approaches have been established previously in plant communities (e.g.,

74   **McGill et al. 2006**), and more recently, **Malik et al. (2020)** proposed a trait-based framework that

75   emphasizes tradeoffs among three primary life history strategies of microorganisms—Y-A-S

76   (Yield-Acquisition-Stress). On the empirical side, a manipulative experiment in a grassland

77   ecosystem in Southern California attributed a drought legacy in litter decomposition to changes in

78   bacterial composition and associated carbohydrate degradation traits (**Martiny et al. 2017**). This

79   study illustrates the potential to establish trait-based linkages between microbial physiology and

80   community shifts underlying legacies.

81   Based on the Y-A-S framework, drought disturbance should cause cellular physiology and

82   microbial composition to shift toward drought tolerance at the expense of other traits, such as

83   investment in exoenzymes. Persistence of this functional shift could result in a drought legacy that

84   affects organic matter decomposition. With this reasoning, factors that shift microbiomes along

85   the tradeoff between enzyme investment and stress tolerance could alter the magnitude and

86   duration of drought legacies. For instance, the intensity of drought, which directly modulates

87   intracellular metabolic allocation to enzymes versus osmolytes (e.g., **Csonka 1989; Schimel 2007**),

88   may determine movement along the tradeoff and hence affect the legacy magnitude. In addition,

89   microbial dispersal (e.g., **Fukami 2015; Vila et al. 2019**) may alter drought legacies through

90   effects on community composition and dynamics that regulate drought-tolerance tradeoffs

91   (**Hawkes et al. 2017**). Therefore, we hypothesize that trait-based tradeoffs between drought

92   tolerance and enzyme investment govern drought legacies in soil microbiomes.

93   Theory-driven, trait-based models are well positioned to complement lab- and field-based

94   studies and test the mechanisms underpinning soil microbiome drought legacies. Individual-based

95   models in particular offer the ability to bridge scales from individual cells through communities to

96   ecosystems by explicitly simulating intra-cellular metabolic processes, ecological dynamics of

97   microbial communities, and emergent functioning (**Allison 2012**). Such an approach can overcome

98   some of the limitations of aggregated models that treat microbes as a single biomass pool or a few

99   discrete functional groups [see a review by **Wieder et al. (2015**)]. In addition, trait- and individual-

100 based models are appropriate for testing the null hypothesis that representing legacies would have

101 little impact on biogeochemical model predictions (**Rousk et al. 2013**).

102   The goal of our study was to analyze the trait-based, tradeoff-mediated mechanisms

103 underpinning drought legacies in soil microbiomes. Our approach applied a modelling framework

104 for soil microbial systems—DEMENTpy—that represents tradeoffs among resource acquisition

105 and drought tolerance at the physiological level along with emergent processes at the community

106 level. This individual- and trait-based model represents physiological mechanisms in a spatially-

107 explicit context. Specifically, we asked the following questions: 1) How does the magnitude of

108 drought legacy vary with drought intensity for the process of litter decomposition? 2) How does

109 microbial dispersal affect the duration and magnitude of drought legacy? 3) What are the

110 underlying changes in enzyme investment and drought tolerance traits? And 4) how do these

111 changes align with the mechanisms proposed in the Y-A-S framework? We tackled these questions

112 by applying DEMENTpy to a grassland ecosystem in Southern California. Our study exemplifies

113 how trait-based investigations into microbiome legacies can improve mechanistic understanding

114 of element cycling in response to climate change.

115

116 **2 Methods**

2.1 Model description

DEMENTpy (DEcomposition Model of ENzymatic Traits in Python; GitHub Repository: https://github.com/bioatmosphere/DEMENTpy) is a spatially-explicit, trait- and individual-based model. Starting from continuous physiological traits, DEMENTpy bridges across soil microbiome scales from individual cells through communities to systems (see **Supporting Fig. 1** for model structure). Its mechanistic modelling framework is built upon its predecessor DEMENT (**Allison 2012; Allison and Goulden 2017; Wang and Allison 2019**). DEMENTpy initiates a microbial community composed by randomly drawing values from uniform distributions of microbial traits and assigning them to a large number of hypothetical taxa (see a list of traits in **Supporting Fig. 1B** and more details in **Supporting Text**). Community dynamics are simulated by explicitly modelling demographic processes of cell metabolism and growth, mortality, and reproduction for each taxon population at a daily time step. Microbial taxa secrete exoenzymes (constitutive and inducible) that degrade different organic compounds at rates that depend on temperature and moisture. To address questions related to drought response, the current version of DEMENTpy represents explicit osmolyte production (constitutive and inducible). Drought tolerance of each taxon is determined by normalizing the inducible osmolyte rate of production to a value from 0 to 1. This formulation establishes a mechanistic connection between osmolyte production and drought tolerance (**Schimel 2007**) in contrast to the previous model version which instead directly introduced a drought tolerance parameter and imposed a corresponding penalty on carbon use efficiency (**Allison and Goulden 2017**).

DEMENTpy tracks intra-cellular metabolism of assimilated monomer carbon derived from exoenzymatic degradation of substrates (**Supporting Fig. 1C**; see **Supporting Text** for substrate degradation and other demographic processes). After growth respiration, assimilated carbon is

7

140 directed to enzyme production, osmolyte production, and associated maintenance respiration,

141 which are treated as simultaneous processes without prescribing an order. The carbon remaining

142 after constitutive and inducible metabolite production accumulates toward biomass (denoted as

143 yield). We assume that constitutive osmolyte production varies across taxa independently of water

144 potential, reflecting microbial allocation to maintain water potential balance across the cell wall

145 (e.g., **Csonka 1989; Potts 1994**). By contrast, inducible production of osmolytes occurs when

146 water potential falls below a threshold. Mortality of microbial cells is simulated both

147 deterministically by accounting for mass balance and stochastically based on death probability

148 dependent on drought tolerance and water potential. More details on model structure, processes,

149 formulae, and parameters are included in the **Supporting Information.**

150 **2.2 Modelling experiments**

151 　　We applied DEMENTpy to a grassland ecosystem at Loma Ridge, Southern California

152 (**Allison et al. 2013**) and parameterized the model with 100 different hypothetical bacterial taxa

153 on a 100 by 100 spatial grid with decomposing grass litter containing ten different substrates (see

154 parameter values in **Supporting Table 1** and substrates in **Supporting Table 2**). DEMENTpy was

155 forced with daily weather data from the year 2011, which is designated as the ambient scenario

156 (**Supporting Fig. 2A**). In addition to this ambient scenario, we conducted simulations to examine

157 drought disturbance response and recovery in three phases (**Supporting Fig. 2**). Two drought

158 scenarios, moderate and severe, were generated by reducing the water potential during the dry

159 season by a factor of four and ten, respectively. After a community establishment phase and a

160 successive drought period, ambient conditions were re-imposed to test for legacy effects on

161 microbial communities and substrate decomposition. Simulations in "default" mode did not allow

162 for microbial dispersal; once taxa disappeared from a default simulation, they could not return. We

163   also ran simulations in "dispersal" mode to test how dispersal affects drought response and legacy

164   effects. In contrast to the default mode, dispersal mode allows extinct taxa to recolonize at the start

165   of each model year. This mode accounts for the possibility that bacterial populations survive in

166   local refugia or nearby wetter areas and then disperse on to fresh litter.

167   **2.3 Simulation protocol**

168   After assigning hypothetical taxa to random locations on a spatial grid with homogeneously

169   distributed substrates, each simulation was run for 10 years at a daily time step (spin-up: 3 years;

170   drought disturbance: 3 years; recovery: 4 years) (**Supporting Fig. 2**). Substrates, monomers, and

171   enzymes were reinitialized uniformly on the spatial grid at the start of each new year at the same

172   concentrations as the first year. At the start of each year, the microbial community on the spatial

173   grid was randomly reinitialized with the same total microbial biomass. Two reinitialization

174   methods were applied to differentiate the default and dispersal modes: for the default mode,

175   microbial community composition was determined according to the fractional biomass of each

176   taxon on the last day of the previous year (**Supporting Fig. 2C**); in dispersal mode, the taxon

177   frequencies were proportional to the cumulative biomass of each taxon over the entire previous

178   year (**Supporting Fig. 2D**). Simulations were repeated 40 times for each scenario under the two

179   modes (default and dispersal) with 40 different random number generation seeds ($5 \times 40 = 200$

180   runs in total). This sample size was determined by a convergence analysis of DEMENTpy's

181   stochastic nature (**Supporting Fig. 3**).

182   **2.4 Data analysis**

183   Unless indicated otherwise, all analyses were conducted on the ensemble of 40 runs for

184   each of the five scenarios. Datasets extracted from these simulations included: taxon traits (enzyme

185   investment and drought tolerance); a time-series of taxon-specific allocation to enzymes (inducible

186   plus constitutive), osmolytes (inducible plus constitutive), carbon yield, and biomass; and a time-

187   series of compound-specific and total substrate concentrations. Taxon-specific allocations to

188   enzymes, osmolytes, and yield were aggregated to derive community-level allocation.

189   Community-level traits of enzyme investment and drought tolerance were calculated from

190   biomass-weighted taxonomic traits (see the **Supporting Text** for calculation method). Because

191   the system stabilized within 3 years (**Supporting Fig. 2**), results up to year 9 (3rd year of recovery

192   from drought disturbance) are presented. In addition, 95% confidence intervals are shown for most

193   variables except for microbial community composition and community carbon allocation, for

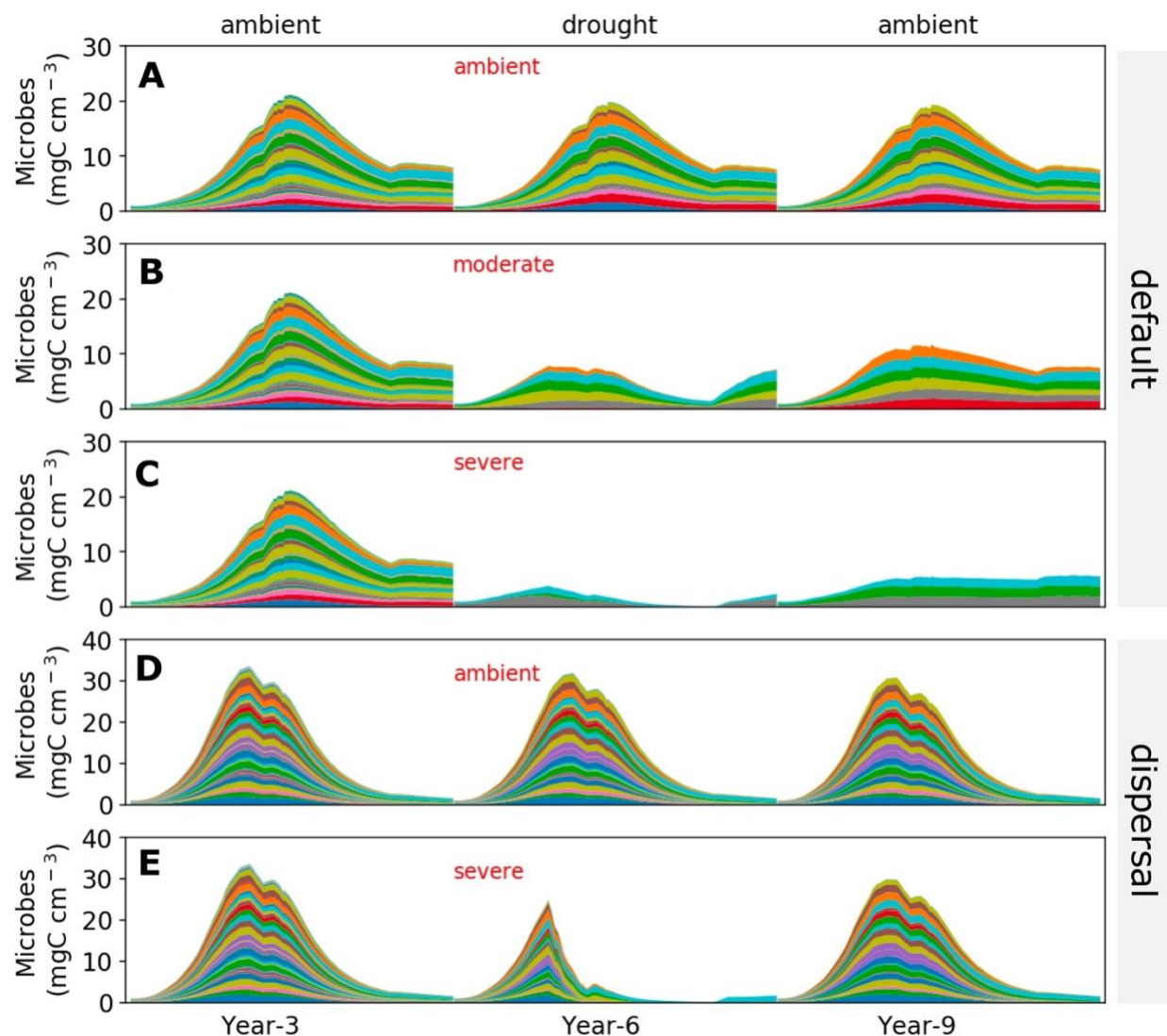194   which only one out of the 40 simulations is shown.

195

Fig. 1. Microbial community dynamics in ambient and drought simulations with and without dispersal. (**A-C**) Dynamics without dispersal under ambient, moderate, and severe drought scenarios, respectively. (**D, E**) Dynamics with dispersal under ambient and severe drought scenarios, respectively. Colored bands represent biomass of hypothetical taxa (mg C cm^{-3}) averaged over the 100×100 spatial grid. Data shown are only for years 3, 6 (the 3rd year under drought), and 9 (the 3rd year after drought). See **Supporting Fig. 2** for the full 10-year dynamics under the ambient scenario of both default and dispersal mode.

3 Results

3.1 Microbial community dynamics under the ambient drought scenario

The system became relatively stable after 2 years, with seasonal dynamics in the microbial community repeating across years (**Supporting Fig. 2**). Seasonal dynamics of community composition and biomass reflected a joint control by climate and substrates. Starting in the wet season that was replete with substrates, the microbial community established and grew in biomass. As substrates were degraded and depleted, microbial cells began to starve and die. Declining water potentials after the start of the dry season induced more death. Together, these two processes resulted in declining microbial biomass from a peak around 20 mg C cm^{-3} (**Fig. 1A)** and drove the composition toward taxa with higher drought tolerance and lower enzyme investment (**Supporting Fig. 4A**). Hence community level enzyme investment decreased (**Fig. 2A**), and drought tolerance increased across the dry season (**Fig. 2B**). Similar seasonal and inter-annual dynamics were observed for the community with dispersal but with higher biomass (peaking around 30 mg C cm^{-3}) and taxonomic diversity (**Fig. 1D; Fig. 2C, D; Supporting Fig. 4B**).
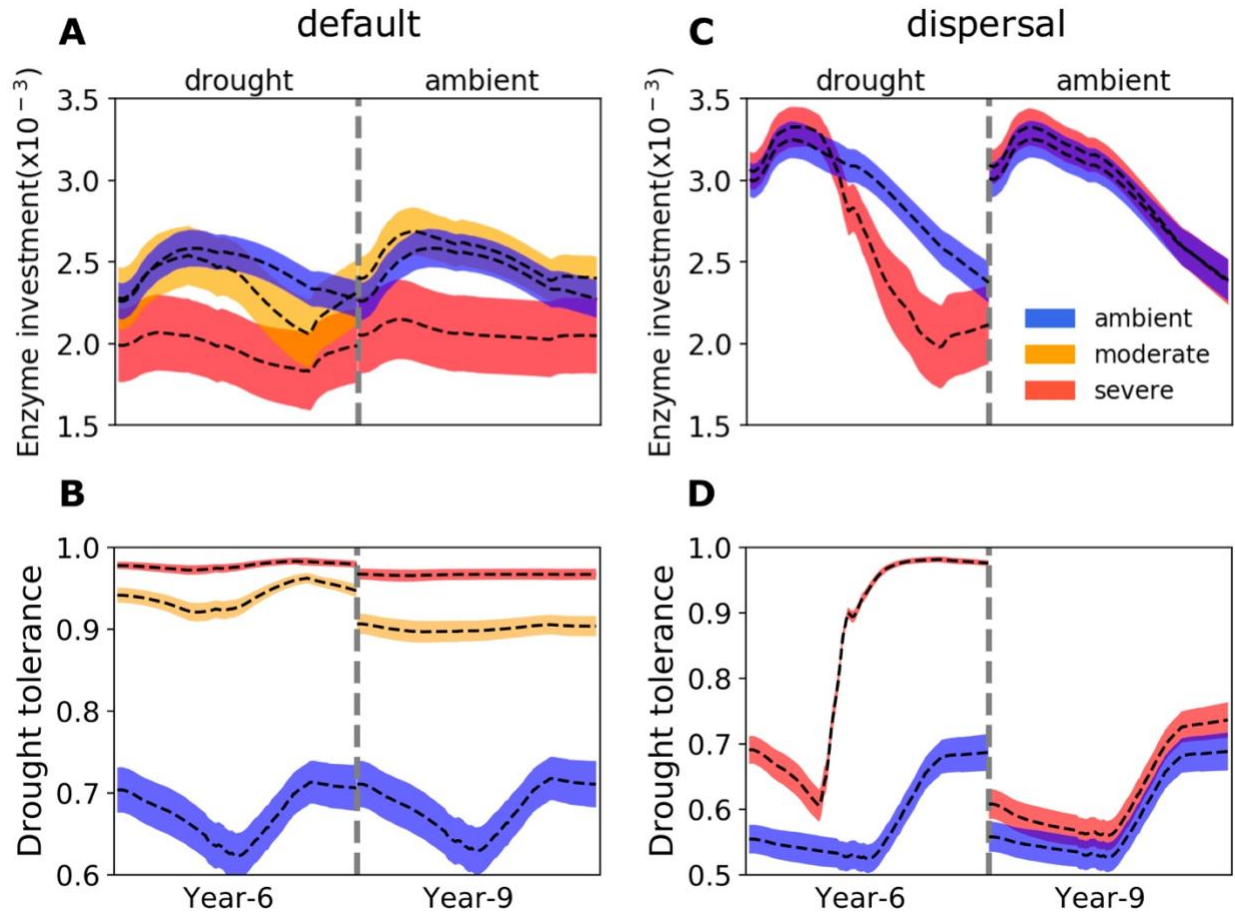
Fig. 2 Seasonal dynamics of community-level enzyme investment and drought tolerance of microbial communities under different drought scenarios. (**A, B**) Enzyme investment and drought tolerance during year 6 (3rd year under drought) and year 9 (3rd year after drought) under three drought scenarios (ambient, moderate, and severe) without dispersal, respectively. (**C, D**) The same for communities with dispersal under two drought scenarios (ambient and severe). Dashed lines and color bands are means and 95% confidence intervals (n = 40).

3.2 Responses to drought disturbance of varying severity

Total microbial biomass declined significantly under drought, with the greatest declines of nearly 50% under the severe scenario, resulting in a peak biomass less than 10 mg C cm^{-3} (**Fig.**

230 **1B, C**). Severe drought also more drastically altered microbial community composition compared

231 to moderate drought. Community taxonomic richness and functional capacity shifted dramatically

232 after 2 years of drought perturbation. Compared to the ambient scenario, drought tolerance

233 increased significantly across seasons from 0.62 up to 0.92 under the moderate scenario and up to

234 0.97 under the severe scenario (**Fig. 2A,B**). However, the community-averaged enzyme

235 investment only declined significantly in the severe scenario across the dry season and did not

236 change substantially in the moderate scenario except late in the dry season (**Fig. 2A,B**). These trait

237 changes reflected differences in community-level carbon allocation between enzymes and

238 osmolytes and thus yield (**Fig. 3A; Supporting Fig. 5A**). Under the moderate drought scenario,

239 the percentage of assimilated carbon allocated to osmolytes ranged between 65% and 85%,

240 compared to the ambient range of 50% to 70%, whereas enzyme allocation was consistently lower

241 (10% on average) compared to the ambient scenario (20% on average). However, the resulting

242 yield was similar, ranging between 0 and 30%, although some days in the ambient scenario were

243 higher (reaching at most 40%) early in the drought season. Under the severe scenario, the

244 allocation to osmolytes was even higher and allocation to enzymes even lower, and the community

245 yield approached zero more often. These differences in community resource allocation resulted in

246 reduced degradation of substrates over the grid, with the two drought scenarios showing different

247 rates of decomposition (average of 57.4% and 85.7%, respectively; **Fig. 4A, B**).
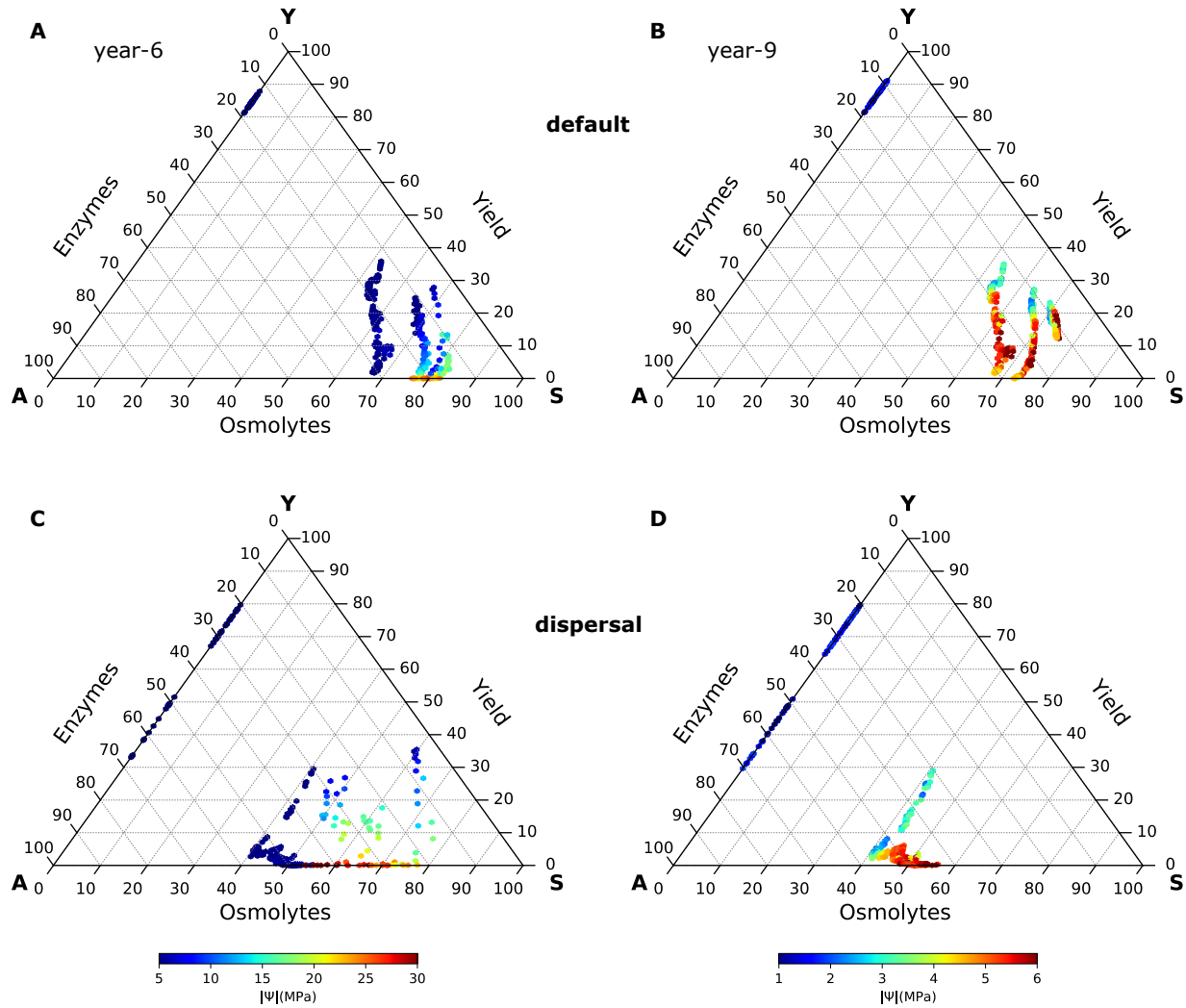
248

249

Fig. 3 Ternary plots of community-level allocation of assimilated carbon among enzymes, osmolytes, and growth yield over time under different dispersal scenarios. (A, B) Enzyme-Osmolyte-Yield tradeoff of communities during year 6 (3rd year under drought) and year 9 (3rd year after drought), respectively, of the default mode (without dispersal). (**C, D**) The same for the dispersal mode. Yield, enzymes, and osmolytes correspond to Y (Yield), A (resource Acquisition), and S (Stress) strategies labeled respectively at the triangle vertices (**Malik et al. 2020**). See **Supporting Fig. 5** for a version with points differentiated by drought scenario instead of water potential.

260   After ambient conditions were re-imposed for 2 years (i.e., by year 9), new stable microbial

261   communities assembled (**Fig. 1B, C** and **Supporting Fig. 2C**). Compared to the ambient scenario,

262   communities that re-assembled following drought had different levels of drought tolerance and

263   enzyme investment. Drought tolerance remained significantly higher under both the moderate

264   drought (0.90) and severe drought (0.96) scenarios, even after drought disturbance ended (**Fig.**

265   **2A**). In contrast, enzyme investment under the moderate scenario became similar to the ambient

266   community, whereas enzyme investment following severe drought remained significantly different

267   (**Fig. 2B**). During the dry season by year 9, only the community that had experienced severe

268   drought showed a clearly lower allocation to enzymes compared to the ambient community (**Fig.**

269   **3B; Supporting Fig. 5B**). The resilience of enzyme investment in the moderate-drought

270   community meant that decomposition rates converged on ambient levels by year 9 (**Fig. 4A**). In

271   contrast, substrate mass loss remained lower by 47.7% on average (**Fig. 4A**) in year 9 of the severe

272   drought scenario, although the magnitude of decline was dampened compared to the antecedent

273   drought period. Prior to year 9, the reductions in mass loss associated with transient microbial

274   communities (year 7) were significant for both drought scenarios (average declines of 18.0% and
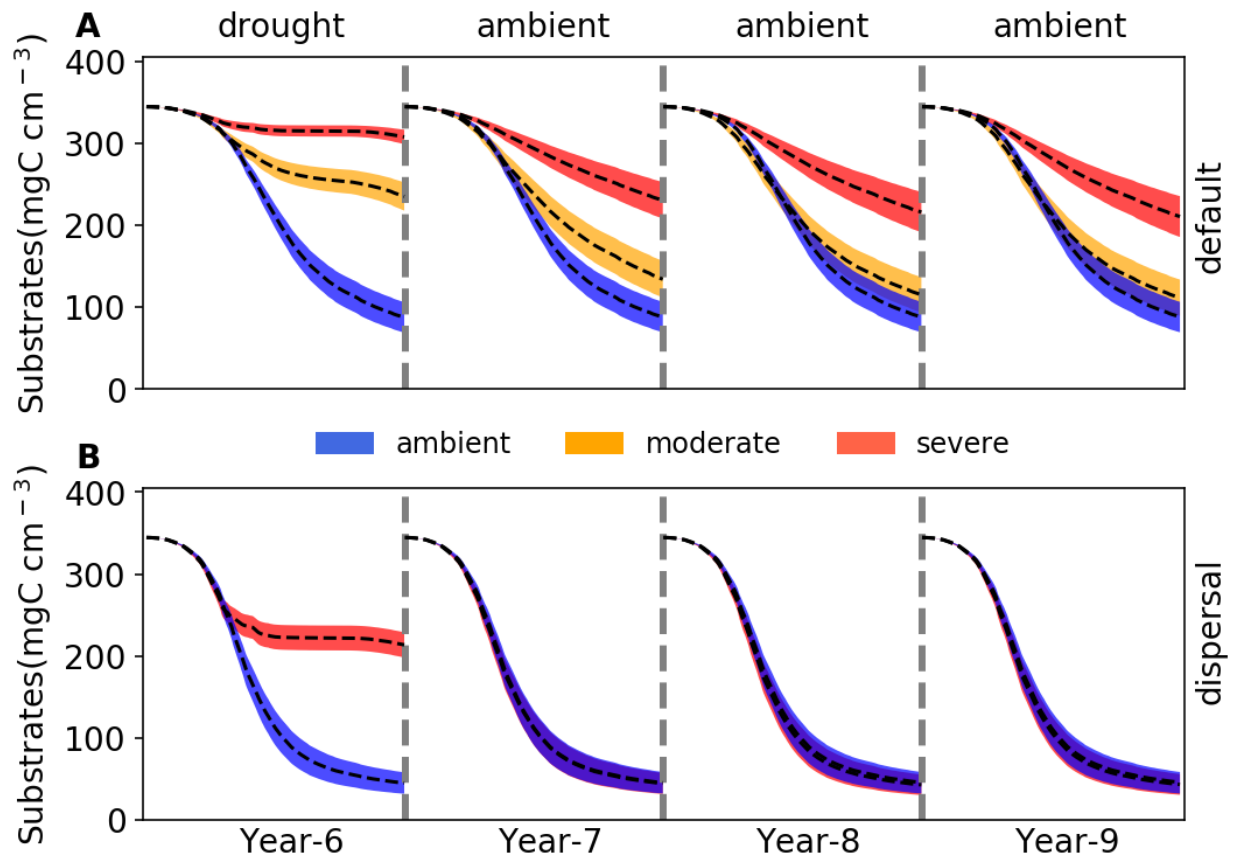
275   55.5%, respectively).

276

277

Fig. 4 Changes in substrate concentrations as litter decomposes during and after drought perturbation. (**A**) Total substrates on the spatial grid during years 6 (last year of drought) to 9 under three different scenarios (ambient, moderate, and severe drought) without dispersal. (**B**) The same for simulations with dispersal under ambient and severe drought scenarios. Dashed lines and colored bands are means and 95% confidence intervals (n = 40), respectively. See **Supporting Fig. 6** for an example illustration of the underlying substrate-specific changes.

3.3 Responses to severe drought disturbance with dispersal

With dispersal of taxa from the previous year's microbial pool, the direct responses to severe drought were similar to the default mode, though with differing magnitudes and seasonal patterns. Compared to ambient conditions, the microbial community showed both lower total

290 biomass and reduced taxonomic richness with drought disturbance, though the values were higher

291 with dispersal than in the default mode (**Fig. 1E**). Community-average enzyme investment and

292 drought tolerance differed between severe drought and ambient scenarios but with a different

293 seasonal pattern predicted for dispersal compared to default mode. With the onset of the dry season,

294 enzyme investment declined sharply from a peak of 0.0033 down to 0.0020, and drought tolerance

295 increased sharply from 0.60 to 0.97, with differences from the ambient scenario increasing over

296 time (**Fig. 2C,D**). These changes reflected the community allocating more assimilated carbon to

297 produce osmolytes and less to enzymes, which resulted in zero yield when drought was most severe

298 during the dry season (**Fig. 3C; Supporting Fig. 5C**). All of these changes resulted in significantly

299 lower substrate decomposition (year 6; an average decline of 56.3%; **Fig. 4A**).

300   When ambient conditions were re-imposed, recovery from drought was rapid with

301 dispersal compared to the default mode. Two years after drought ended, the communities became

302 similar in the drought and ambient scenarios (**Fig. 1E**), a stark contrast to the default mode (**Fig.**

303 **1C**). This compositional similarity coincided with similar community enzyme investment (**Fig.**

304 **2C**) and drought tolerance (**Fig. 2D**), which resulted in the same community-level allocation of

305 assimilated carbon among enzymes (30 - 60%), osmolytes (40 - 60%), and thus yield (0 - 30%;

306 **Fig. 3D; Supporting Fig. 5D**). These communities ultimately had almost exactly the same

307 composition and substrate decomposition rates (**Fig. 4B**). In fact, in contrast to the default mode,

308 the transient community did not even show significant differences in the 1st year following drought

309 (year 7; **Fig. 4B**). Based on this clear lack of legacy effects following severe drought, we did not

310 find it relevant to run simulations of the moderate scenario with dispersal.

311

312 **4 Discussion**

313   By representing physiological mechanisms in a trait-based model, we tested the

314 relationships between drought legacy and drought severity and dispersal in simulated litter

315 microbiomes. Drought legacy effects on litter decomposition ranged from persistent through

316 transient to non-existent and depended on drought severity and microbial dispersal (**Fig. 4**). This

317 variation in legacy magnitude and duration showed a clear mechanistic basis—tradeoffs between

318 enzyme production and drought tolerance, in line with the Y-A-S strategy framework. These

319 results are relevant for understanding the resilience of microbial systems—weaker legacies

320 correspond to higher resilience of soil microbiome functioning in response to historical drought.

321 Our analysis of legacy mechanisms underlying microbial system resilience will help more

322 accurately quantify carbon cycle feedbacks to drought in the Earth system.

323

324 **Transient legacy under moderate drought**

325   The severity of drought disturbance influences legacy magnitude and duration by

326 determining the extent to which a microbial community can adapt (**Fig. 4A**). Our drought

327 disturbance lasted long enough for communities to reach a stable state. However, our simulations

328 focused on testing underlying mechanisms and only represent a subset of actual drought

329 disturbances in terms of frequency, intensity, and duration. At the drought intensities we analyzed,

330 legacies ranged from transient to persistent. Weaker disturbances might result in no legacy at all.

331   Drought of lower severity had a transient negative effect on decomposition post-

332 disturbance, but eventually the legacy effect disappeared (**Fig. 4A**), a pattern that we dub "transient

333 legacy". This transient legacy pattern matches results from a reciprocal transplant experiment with

334 microbial communities from a rainfall manipulation experiment at Loma Ridge, CA. Here, the

drought legacy effect on litter decomposition disappeared after one year (**Martiny et al. 2017**). It is noteworthy that our model-predicted recovery from drought was driven by a community with the same functioning but different composition and biomass. However, with a total biomass difference varying from 50% to almost zero (**Fig. 1B**), microbial biomass is probably not a major driver of the legacy pattern, consistent with findings from Loma Ridge (**Martiny et al. 2017**) and another reciprocal transplant study across a climate gradient in Southern California (**Glassman et al. 2018**). Rather, the transience of the legacy mainly resulted from convergence in community enzyme investment despite lingering differences in community composition and drought tolerance (**Fig. 2A,B**). Such a compositional but not functional change in an ecosystem after disturbance—which has been observed before (e.g., **Fukami 2015; Ives and Carpenter 2007**)—supports the notion of functional similarity in the soil microbiome (**Allison and Martiny 2008; Louca et al. 2018**). This transient legacy mechanism may allow for resilience of microbial and other systems following moderate perturbation.

Persistent legacy under severe drought

A strong drought disturbance can push a community to reach an even higher drought tolerance by sacrificing more investment in enzyme production (including a loss of relatively more drought-intolerant taxa), thereby forming a community not only compositionally but also functionally different (**Fig. 2A,B**). These conditions can lead to a persistent legacy (**Fig. 4B**). A similar long-term legacy in soil heterotrophic respiration has also been observed in microcosm and field transplant experiments (**Hawkes et al. 2017**). This persistent legacy is consistent with the idea of alternative stable states with different functioning in ecological systems (**Scheffer et al. 2001**). Disturbance-driven alternative stable states have been reported across an array of systems;

358 e.g., in gut microbiota experiencing transient osmotic perturbation (**Tropini et al. 2018**) and in

359 tropical (e.g., **Staver et al. 2011**) and boreal forests (**Herzschuh 2020**), as well as in small pond

360 systems (**Chase 2003**). Conceptually, a persistent legacy means the loss of system resilience with

361 severe disturbance (**Scheffer et al. 2001**).

362

363 **Disappearance of legacy under severe drought with dispersal**

364   Importantly, dispersal can reduce legacies in organic matter decomposition (**Fig. 4B**). By

365 re-introducing taxa from the previous year's microbial pool, we found that even with severe

366 drought, dispersal can rescue taxa from extinction and completely mitigate the effect of

367 environmental selection on the microbial community (**Fig. 1E**). By restoring drought tolerance

368 and enzyme investment traits (**Fig. 2C,D; Fig. 3D**), dispersal can overwhelm the drought legacy

369 in organic matter decomposition (**Fig. 4B**). This result suggests that dispersal can increase

370 microbial systems' resilience to drought disturbance (**Allison and Martiny 2008**) in stark contrast

371 to the persistent legacy induced by severe drought disturbance without dispersal (**Fig. 4A**). We

372 note that there are many dispersal factors that influence community dynamics but were not

373 represented in our model. For instance, dispersal timing (e.g., priority effects) and magnitude both

374 matter for community response to perturbation (e.g., **Fukami 2015; Vila et al. 2019**). Furthermore,

375 even an unsuccessful invasion by a single species that interacts only briefly with the resident

376 community can induce an alternative stable state with distinct functioning (**Amor et al. 2020**).

377 Variation in dispersal processes could therefore drive compositional and functional changes to

378 varying extents (e.g., **Fukami 2015**), resulting in varying magnitudes of decomposition legacy.

379 For example, in a field transplant experiment with passive dispersal, **Hawkes et al. (2017)** did not

380 find apparent mitigation of historical rainfall legacy in soil respiration. Given this result, we

381   recognize that our exploration of dispersal mechanisms and intensities is incomplete; our study

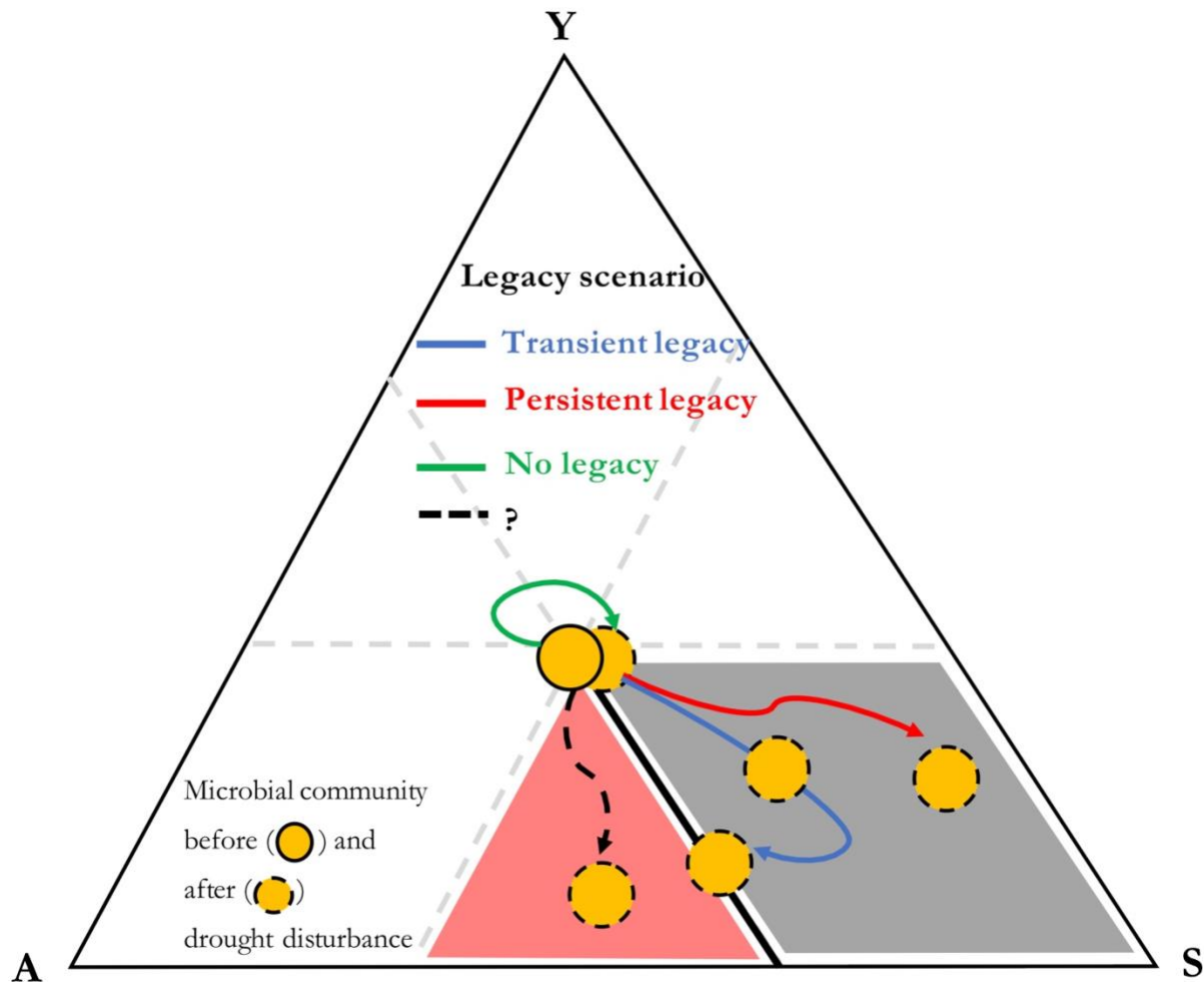382   was mainly aimed at revealing underlying mechanisms and not meant to be exhaustive.

383

384   **Fig. 5 Overlay of drought legacy scenarios in YAS-constrained space.** Drought legacy is

385   contingent on the trajectory of a microbial community in the YAS space after drought disturbance.

386   There will be no legacy if a community does not move at all (green trajectory) or if it moves along

387   the thick black line. If an altered community remains in the grey region, a persistent legacy will

388   occur. However, if the community eventually leaves the grey region and returns to the thick black

389   line, a transient legacy can occur. We also propose that a community could move into the red

390   region with both increased drought tolerance and enzyme investment (but at the expense of growth

22

391 yield). Note: the positioning of the starting community in the center of the space (filled yellow

392 circle) is for illustration purposes only; real communities may start anywhere in the YAS space.

393

394 **A mechanistic conceptual framework**

395   We propose to organize legacy scenarios based on the YAS framework, as illustrated in

396 **Fig. 5**. Drought legacies are ultimately determined by the trajectory of a community in a conceptual

397 space defined by enzyme investment, drought tolerance, and yield. Factors that affect cellular

398 metabolic and community-level tradeoffs between enzyme and osmolyte production may influence

399 the magnitude and/or duration of a drought legacy. For instance, when drought selects for a

400 community with higher drought tolerance but ultimately similar enzyme investment (e.g.,

401 moderate drought scenario; **Fig. 4A**), a transient legacy occurs. However, when more severe

402 drought selects for higher drought tolerance at the expense of enzyme investment (**Fig. 4A**), a

403 persistent legacy with impaired substrate decomposition can occur. In contrast, when the

404 community does not shift in strategy space (e.g., with dispersal present; **Fig. 4B**), even transient

405 legacies may not occur.

406   Tradeoffs in microbiomes and the biosphere more generally are often complex (e.g.,

407 **Berezovsky & Shakhnovich 2005; Ferenci 2016**). Some tradeoffs may be context-specific, and

408 even positive relationships between costly traits may be observed under certain conditions

409 (**Moreno-Gámez et al. 2020; Tikhonov et al. 2020**). These principles may apply to the

410 relationship between enzyme investment and drought tolerance which may depend on drought

411 intensity, dispersal, metabolic plasticity, and evolution history. For instance, a fourth legacy

412 scenario may exist with both increased osmolyte and enzyme investment that trade off against

413 lower yield (the red region in **Fig. 5**). Going forward, our study could be extended by broadening

414   the range of drought and dispersal scenarios and modifying the tradeoff assumptions in

415   DEMENTpy to gain a more complete picture of the mechanisms underlying drought legacies.

416

417   **Implications**

418   Our study revealed a tradeoff-mediated explanation for community-level trait changes that

419   leads to drought legacies in soil microbiomes. This mechanistic insight has consequences for

420   ecosystem responses to drought and other environmental changes. A more accurate quantification

421   of the magnitude and duration of drought legacies should enable better predictions of litter and soil

422   organic matter decomposition. Legacies of impaired decomposition, even when transient, may

423   enhance carbon sequestration in soil systems, but may also allow fuels to accumulate for the next

424   fire season, thereby increasing fire risk (e.g., **Pellegrini et al. 2018**). Additionally, impaired

425   decomposition can inhibit nutrient turnover and availability, thereby influencing plant productivity

426   and interactions with microbes (e.g., **Kaisermann et al. 2017**). These and other cascading changes

427   arising from microbiome legacies could initiate more complex ecosystem feedbacks. Evaluating

428   these implications requires a holistic approach that integrates microbial and vegetation processes

429   across ecosystem to Earth system scales. Such an approach is crucial for predicting

430   biogeochemical rates in the context of projected global climate change that may induce legacy

431   effects. Trait-based models of both microbial and vegetation dynamics are proving essential in

432   achieving this predictive understanding.

433

434   **References**

435   Allison, S. D. (2012). A trait-based approach for modelling microbial litter decomposition.

436   Ecology Letters, 15, 1058-1070.

437

438 Allison, S. D., & Goulden, M. L. (2017). Consequences of drought tolerance traits for microbial

439 decomposition in the DEMENT model. Soil Biology and Biochemistry, 107, 104-113.

440

441 Allison, S. D., Lu, Y., Weihe, C., Goulden, M. L., Martiny, A. C., Treseder, K. K., & Martiny, J.

442 B. (2013). Microbial abundance and composition influence litter decomposition response to

443 environmental change. Ecology, 94, 714-725.

444

445 Allison, S. D., & Martiny, J. B. (2008). Resistance, resilience, and redundancy in microbial

446 communities. Proceedings of the National Academy of Sciences, 105, 11512-11519.

447

448 Amor, D. R., Ratzke, C., & Gore, J. (2020). Transient invaders can induce shifts between

449 alternative stable states of microbial communities. Science Advances, 6, eaay8676.

450

451 Anderegg, W. R., Schwalm, C., Biondi, F., Camarero, J. J., Koch, G., Litvak, M., ... & Wolf, A.

452 (2015). Pervasive drought legacies in forest ecosystems and their implications for carbon cycle

453 models. Science, 349, 528-532.

454

455 Berdugo, M., Delgado-Baquerizo, M., Soliveres, S., Hernández-Clemente, R., Zhao, Y., Gaitán, J.

456 J., ... & Rillig, M. C. (2020). Global ecosystem thresholds driven by aridity. Science, 367, 787-

457 790.

458

459   Berezovsky, I. N., & Shakhnovich, E. I. (2005). Physics and evolution of thermophilic adaptation.

460   Proceedings of the National Academy of Sciences, 102, 12742-12747.

461

462   Birch, H. F. 1958. The effect of soil drying on humus decomposition and nitrogen availability.

463   Plant and Soil, 10, 9–31.

464

465   Borsa, A. A., Agnew, D. C., & Cayan, D. R. (2014). Ongoing drought-induced uplift in the western

466   United States. Science, 345, 1587-1590.

467

468   Conradi, T., Van Meerbeek, K., Ordonez, A., & Svenning, J. C. (2020). Biogeographic historical

469   legacies in the net primary productivity of Northern Hemisphere forests. Ecology Letters, 23, 800-

470   810.

471

472   Csonka, L. N. (1989). Physiological and genetic responses of bacteria to osmotic stress.

473   Microbiological Reviews, 53, 121-147.

474

475   Cuddington, K. (2011). Legacy Effects: The Persistent Impact of Ecological Interactions.

476   Biological Theory, 6, 203–210.

477

478   Evans, S.E., Wallenstein, M.D. (2012) Soil microbial community response to drying and rewetting

479   stress: does historical precipitation regime matter? Biogeochemistry, 109, 101–116.

480

481 Evans, S. E., & Wallenstein, M. D. (2014). Climate change alters ecological strategies of soil

482 bacteria. Ecology Letters, 17, 155-164.

484 Falkowski, P. G., Fenchel, T., & Delong, E. F. (2008). The microbial engines that drive Earth's

485 biogeochemical cycles. Science, 320, 1034-1039.

487 Ferenci, T. (2016). Trade-off mechanisms shaping the diversity of bacteria. Trends in

488 Microbiology, 24, 209-223.

490 Fuchslueger, L., Bahn, M., Hasibeder, R., Kienzl, S., Fritz, K., Schmitt, M., ... & Richter, A. (2016).

491 Drought history affects grassland plant and microbial carbon turnover during and after a

492 subsequent drought event. Journal of Ecology, 104, 1453-1465.

494 Fukami, T. (2015). Historical contingency in community assembly: integrating niches, species

495 pools, and priority effects. Annual Review of Ecology, Evolution, and Systematics, 46, 1-23.

497 Glassman, S. I., Weihe, C., Li, J., Albright, M. B., Looby, C. I., Martiny, A. C., ... & Martiny, J.

498 B. (2018). Decomposition responses to climate depend on microbial community composition.

499 Proceedings of the National Academy of Sciences, 115, 11994-11999.

501 Green, J.K., Seneviratne, S.I., Berg, A.M. *et al.* (2019). Large influence of soil moisture on long-

502 term terrestrial carbon uptake. Nature, 565**,** 476–479.

504   Hawkes, C. V., & Keitt, T. H. (2015). Resilience vs. historical contingency in microbial responses

505   to environmental change. Ecology Letters, 18, 612-625.

506

507   Hawkes, C. V., Waring, B. G., Rocca, J. D., & Kivlin, S. N. (2017). Historical climate controls

508   soil respiration responses to current soil moisture. Proceedings of the National Academy of

509   Sciences, 114, 6322-6327.

510

511   Herzschuh, U. (2020). Legacy of the Last Glacial on the present-day distribution of deciduous

512   versus evergreen boreal forests. Global Ecology and Biogeography, 29, 198-206

513

514   Hinojosa, M. B., Laudicina, V. A., Parra, A., Albert-Belda, E., & Moreno, J. M. (2019). Drought

515   and its legacy modulate the post-fire recovery of soil functionality and microbial community

516   structure in a Mediterranean shrubland. Global Change Biology, 25, 1409-1427.

517

518   Ives, A. R., & Carpenter, S. R. (2007). Stability and diversity of ecosystems. Science, 317, 58-62.

519

520   Kaisermann, A., de Vries, F. T., Griffiths, R. I., & Bardgett, R. D. (2017). Legacy effects of

521   drought on plant–soil feedbacks and plant–plant interactions. New Phytologist, 215, 1413-1424.

522

523   Karhu, K., Auffret, M., Dungait, J. et al. (2014) Temperature sensitivity of soil respiration rates

524   enhanced by microbial community response. Nature, 513, 81–84

525

526 Louca, S., Polz, M.F., Mazel, F. et al. (2018). Function and functional redundancy in microbial

527 systems. Nature Ecology Evolution, 2, 936–943.

528

529 Malik, A.A., Martiny, J.B.H., Brodie, E.L. *et al.* (2020). Defining trait-based microbial strategies

530 with consequences for soil carbon cycling under climate change. ISME J 14, 1–9.

531

532 Manzoni, S., Schimel, J. P., & Porporato, A. (2012). Responses of soil microbial communities to

533 water stress: results from a meta-analysis. Ecology, 93, 930-938.

534

535 Martiny, J., Martiny, A., Weihe, C. et al. (2017). Microbial legacies alter decomposition in

536 response to simulated global change. ISME J 11, 490–499.

537

538 McGill, B. J., Enquist, B. J., Weiher, E., & Westoby, M. (2006). Rebuilding community ecology

539 from functional traits. Trends in Ecology & Evolution, 21, 178-185.

540

541 Meisner, A., Rousk, J., & Bååth, E. (2015). Prolonged drought changes the bacterial growth

542 response to rewetting. Soil Biology and Biochemistry, 88, 314-322.

543

544 Moreno-Gámez, S., Kiviet, D. J., Vulin, C., Schlegel, S., Schlegel, K., van Doorn, G. S., &

545 Ackermann, M. (2020). Wide lag time distributions break a trade-off between reproduction and

546 survival in bacteria. Proceedings of the National Academy of Sciences, 117, 18729-18736.

547

548 Pellegrini, A., Ahlström, A., Hobbie, S. *et al.* (2018). Fire frequency drives decadal changes in soil

549 carbon and nitrogen and ecosystem productivity. Nature, 553**,** 194–198.

550

551 Potts, M. (1994). Desiccation tolerance of prokaryotes. Microbiological Reviews, 58, 755-805.

552

553 Rousk, J., Smith, A. R., & Jones, D. L. (2013). Investigating the long-term legacy of drought and

554 warming on the soil microbial community across five European shrubland ecosystems. Global

555 Change Biology, 19, 3872-3884.

556

557 Scheffer, M., Carpenter, S., Foley, J. A., Folke, C., & Walker, B. (2001). Catastrophic shifts in

558 ecosystems. Nature, 413, 591-596.

559

560 Schimel, J., Balser, T. C., & Wallenstein, M. (2007). Microbial stress-response physiology and its

561 implications for ecosystem function. Ecology, 88, 1386-1394.

562

563 Staver, A. C., Archibald, S., & Levin, S. A. (2011). The global extent and determinants of savanna

564 and forest as alternative biome states. Science, 334, 230-232.

565

566 Tikhonov, M., Kachru, S., & Fisher, D. S. (2020). A model for the interplay between plastic

567 tradeoffs and evolution in changing environments. Proceedings of the National Academy of

568 Sciences, 117, 8934-8940.

569

570 Tropini, C., Moss, E. L., Merrill, B. D., Ng, K. M., Higginbottom, S. K., Casavant, E. P., ... &

571 Bhatt, A. S. (2018). Transient osmotic perturbation causes long-term alteration to the gut

572 microbiota. Cell, 173, 1742-1754.

573

574 Wang, B., & Allison, S. D. (2019). Emergent properties of organic matter decomposition by soil

575 enzymes. Soil Biology and Biochemistry, 136, 107522.

576

577 Waring, B., Hawkes, C. V. (2018). Ecological mechanisms underlying soil bacterial responses to

578 rainfall along a steep natural precipitation gradient, FEMS Microbiology Ecology, 94, fiy001.

579

580 Vila, J. C., Jones, M. L., Patel, M., Bell, T., & Rosindell, J. (2019). Uncovering the rules of

581 microbial community invasions. Nature Ecology & Evolution, 3, 1162-1171.

582

583 Wieder, W. R., Allison, S. D., Davidson, E. A., Georgiou, K., Hararuk, O., He, Y., ... & Todd-

584 Brown, K., 2015. Explicitly representing soil microbial processes in Earth system models. Global

585 Biogeochemical Cycles, 29, 1782-1800.

586

587 **Acknowledgements**

Supporting Information

Drought Legacies Mediated by Trait Tradeoffs in Soil Microbiomes

3   Bin Wang [1], Steven D. Allison [1,2]

4   [1] Department of Ecology and Evolutionary Biology, University of California, Irvine, CA

5   [2] Department of Earth System Science, University of California, Irvine, CA

6

1 DEMENTpy

DEMENTpy is a trait-based modelling framework with spatially-explicit representation of individual populations in microbial communities. The model version reported here updates the physiological mechanisms (see **Supporting Fig. 1** for conceptual structure) and programming approach (see **Supporting Fig. 7** for programming structure) to the DEMENT model that was initially developed in 2012 (**Allison 2012**). The source code in Python is accessible at https://github.com/bioatmosphere/DEMENTpy. Processes simulated in DEMENTpy are described below.

1.1 Microbial community initialization

Using a trait-based approach, DEMENTpy initiates a microbial pool with a large number of hypothetical taxa by randomly drawing values from distributions of physiological traits (**Supporting Table 1**) and assigning them to different taxa. These hypothetical taxa in the microbial pool with differing combinations of trait values are randomly placed on the spatial grid to form a spatially structured microbial community. Illustrative animations are available at https://bioatmosphere.github.io/DEMENTpy/, and see **Wang and Allison (2019)** for an application of model spatial resolution for scaling up enzymatic heterogeneity. Trait distributions are all assumed to follow uniform distributions, except that for simplicity, some trait values are

24 assumed to be constant, and values of some traits are derived from established correlations with

25 other traits. These distributions and assumptions are largely informed by field- and lab-based

26 empirical studies (**Allison 2012; Allison and Goulden 2017**).

27   The key traits determining mass balance in drought simulations are constitutive and

28 inducible rates of enzyme and osmolyte production. The richness of genes encoding different

29 enzymes and osmolytes is determined randomly for each taxon during model initialization.

30 Therefore, gene richness and production rate together determine the amounts of enzyme and

31 osmolyte a cell can produce. The rate of inducible osmolyte production is then normalized to a

32 value from 0 to 1, which is regarded as drought tolerance. This parameterization of drought

33 tolerance is an update to the previous DEMENT version which instead directly introduced a

34 drought tolerance parameter and imposed a penalty on carbon use efficiency (**Allison and**

35 **Goulden 2017**). Linking osmolyte production directly to drought tolerance is intended to be more

36 biologically realistic (**Schimel 2007**). Additionally, kinetic traits including *Vmax* and *Km* are

37 assigned to explicitly parameterize a certain number of different enzymes and transporters in the

38 model system.

39 **1.2 Metabolic production of enzyme and osmolyte**

40   Different individuals (hypothetical taxa) comprising the microbial community undergo

41 demographic processes of growth, mortality, and reproduction while degrading substrates and

42 assimilating monomers at rates dependent on temperature and water potential. From these

43 underlying processes emerge dynamics and functioning at both the microbial cell level and the

44 whole system level.

45   Substrate degradation rates are calculated based on the activities of enzymes with different

46 kinetic properties. Every enzyme degrades at least one substrate, and every substrate is degraded

47   by at least one enzyme. Monomer uptake is calculated based on transporter abundance and kinetic

48   traits which are specific to each taxon. The governing equation for both substrate degradation and

49   monomer uptake follows the Michaelis-Menten equation, which is constrained by temperature

50   (accounting for temperature impacts on enzymatic kinetics) and water potential (accounting for

51   moisture constraints on enzymatic kinetics and diffusion; **Allison and Goulden 2017**):

52
$$V = \frac{V_{max}f(T)[S][E]}{K_m+[S]} f(\psi)$$

53
$$f(T) = e^{\left(-\frac{\varepsilon}{R}\left(\frac{1}{T}-\frac{1}{T_{ref}}\right)\right)}$$

54
$$f(\psi) = e^{k\psi}$$

55   where E and S are matrices containing enzyme and substrate concentrations, respectively, $Vmax$

56   represents the enzyme catalytic constant, K_m denotes the concentration of S at which V is one half

57   V_{max}, ε is enzymatic activation energy, R is universal gas constant, and k is a coefficient controlling

58   water potential sensitivity that differs between degradation and uptake.

59   Cellular metabolism balances carbon upon uptake from degraded substrates and carbon

60   loss through constitutive and inducible metabolite production (**Supporting Fig. 1C**). After growth

61   respiration (constrained by a constant), assimilated carbon is directed to enzyme and osmolyte

62   production along with their associated maintenance respiration rates, all of which are treated

63   simultaneously in the model without prescribing an order. The carbon remaining after these

64   processes accumulates toward biomass. We assume the constitutive osmolyte production rate

65   (*Osmo_Con*) varies across taxa independent of water potential, accounting for microbial allocation

66   to maintain water potential balance across the cell wall (**Csonka 1989; Potts 1994**). In contrast,

67   taxon-specific inducible production of osmolytes (*O_{ind}*) depends on water potential as follows:

68

69
$$O_{ind}(i) = \begin{cases} O_{ind}(i), & \psi \geq \psi_{th} \\ O_{ind}(i)\,(1 - \alpha\psi), & \psi < \psi_{th} \end{cases}$$

70

71   where O_{ind}, is the ith taxon's inducible osmolyte production rate, ψ is the daily water potential, α

72   is a coefficient determining water potential sensitivity, and ψ_{th} is a system water potential constant,

73   below which inducible osmolyte production is activated. Osmolyte stoichiometry is assumed to be

74   constant at C/N = 3, which governs consumption of N in intracellular metabolism. This ratio is

75   based on an average of the three most common osmotic compounds in bacteria (**Csonka 1989;**

76   **Potts 1994**): proline ($C_5H_9NO_2$), glycine betaine ($C_5H_{11}NO_2$), and glutamine ($C_5H_{10}N_2O_3$).

77   Mortality of microbial cells is simulated both deterministically by accounting for mass

78   balance relative to a threshold, and stochastically based on a death probability constrained by

79   drought tolerance and water potential. Here the taxon-specific mortality probability (*Mort*) is

80   calculated as:

81

82    $$Mort_i = Death\_basal_i[1 - Death\_rate_i(1 - Tol_i)(\psi - \psi_{th})\,]$$

83

84   where *Death_basal* is the ith taxon's basal mortality probability, *Death_rate* is a death probability

85   coefficient controlling water potential sensitivity, *Tol* is the ith taxon's drought tolerance, and ψ_{th}

86   is a system water potential constant. Microbial cells that fall below the biomass threshold or that

87   die randomly are removed from the microbial community and added into the substrate pools as

88   dead microbes. Microbial reproduction is calculated by splitting microbes into two equal halves,

89   followed by local dispersal to surrounding grid boxes on the spatial grid (**Allison 2012**).

90

91 **2. Calculation of community-level traits**

92   Community-level enzyme investment (E_{com}) and drought tolerance (D_{com}) weighted by

93 biomass are calculated as:

$$E_{com} = \sum_{i}^{n} EiMi$$

94

$$D_{com} = \sum_{i}^{n} DiMi$$

95

96

97 respectively, where Ei and Di refer to the ith taxon's enzyme production rate and drought tolerance,

98 respectively, and Mi is the relative biomass of the ith taxon in the community.

99

100 **References**

101 Allison, S. D. (2012). A trait-based approach for modelling microbial litter decomposition.

102 Ecology letters, 15, 1058-1070.

103

104 Allison, S. D., & Goulden, M. L. (2017). Consequences of drought tolerance traits for microbial

105 decomposition in the DEMENT model. Soil Biology and Biochemistry, 107, 104-113.

106

107 Bugmann, H., Fischlin, A., & Kienast, F. (1996). Model convergence and state variable update in

108 forest gap models. Ecological Modelling, 89, 197-208.

109

110 Csonka, L. N. (1989). Physiological and genetic responses of bacteria to osmotic stress.

111 Microbiological Reviews, 53, 121-147.

112

113   Potts, M. (1994). Desiccation tolerance of prokaryotes. Microbiological Reviews, 58, 755-805.

114

115   Schimel, J., Balser, T. C., & Wallenstein, M. (2007). Microbial stress-response physiology and its

116   implications for ecosystem function. Ecology, 88, 1386-1394.

117

118   Wang, B., & Allison, S. D. (2019). Emergent properties of organic matter decomposition by soil

119   enzymes. Soil Biology and Biochemistry, 136, 107522.

Supporting Table 1 Microbial and enzyme parameters and their values

Parameter	Value	Unit	Note
max_size_b	2	mg cm-3	C quota threshold for bacterial cell division
Cfrac_b	0.825	mg mg-1	Bacterial C fraction
Nfrac_b	0.16	mg mg-1	Bacterial N fraction
Pfrac_b	0.015	mg mg-1	Bacterial P fraction
Crange	0.09	mg mg-1	Tolerance on C fraction
Nrange	0.04	mg mg-1	Tolerance on N fraction
Prange	0.005	mg mg-1	Tolerance on P fraction
C_min	0.086	mg cm-3	Threshold C concentration for cell death
N_min	0.012	mg cm-3	Threshold P concentration for cell death
P_min	0.002	mg cm-3	Threshold C concentration for cell death
Uptake_C_cost_min	0.01	transporter mg-1 biomass C	Minimun per enzyme C cost as a fraction of uptake
Uptake_C_cost_max	0.1	transporter mg-1 biomass C	Maximum per enzyme C cost as a fraction of uptake
Uptake_Maint_cost	0.01	mg C transporter-1 day-1	Respiration cost of uptake transporters
Enz_per_taxon_min	0		Minimum number of enzymes a taxon can produce
Enz_per_taxon_max	40		Maximum number of enzymes a taxon can produce
Enz_Prod_min	0.00001	mg C mg-1 day-1	Minimum per enzyme production cost as a fraction of C uptake rate
Enz_Prod_max	0.0001	mg C mg-1 day-1	Maximum per enzyme producton cost as a fraction of C uptakte rate
Constit_Prod_min	0.00001	mg C mg-1 day-1	Minimum per enzyme production cost as a fraction of biomass C
Constit_Prod_max	0.0001	mg C mg-1 day-1	Maximum per enzyme production cost as a fraction of biomass C
Osmo_per_taxon_min	1		Minimum number of osmolyte a taxon can produce
Osmo_per_taxon_max	1		Maximum number of osmolyte a taxon can produce
Osmo_Consti_Prod_min	0.0000001	mg C mg-1 day-1	Minimum per osmolyte production cost as a fraction of biomass C
Osmo_Consti_Prod_max	0.000001	mg C mg-1 day-1	Maximum per osmolyte production cost as a fraction of biomass C
Osmo_Induci_Prod_min	0.01	mg C mg-1 day-1	Minimum per osmolyte production cost as a fraction of C uptake rate
Osmo_Induci_Prod_max	0.1	mg C mg-1 day-1	Maximum per osmolyte production cost as a fraction of C uptake rate
CUE_ref	0.5	mg mg-1	Growth efficiency at the reference temperature
CUE_temp	-0.005	mg mg-1	Growth efficiency change with enzyme investment
death_rate_bac	0.001		Bacterial death rate
basal_bac	10		Bacterial basal death probability
wp_th	-2.00	MPa	Water potential threshold at which osmolyte is induced
alpha	0.01	mg C mg-1 day-1	Osmolyte production change with water potential
Vmax0_min	5	mg substrate mg-1 enzyme day-1	Minimum Vmax for enzyme
Vmax0_max	50	mg substrate mg-1 enzyme day-1	Maximum Vmax for enzyme

Uptake_Vmax0_min	1	mg substrate mg-1 substrate day-1	Minimum uptake Vmax
Uptake_Vmax0_max	10	mg substrate mg-1 substrate day-1	Maximum uptake Vmax
Uptake_Ea_min	35	kj mol-1	Minimum activation energy for uptake
Uptake_Ea_max	35	kj mol-1	Maximum activation energy for uptake
Km_min	0.01	mg cm-3	Minimum Km
Uptake_Km_min	0.001	mg cm-3	Minimum uptake Km
Vmax_Km	1	mg enzyme day cm-3	Slope for Km-Vmax relationship
Vmax_Km_int	0	mg cm-3	Intercept for Km-Vmax relationship
Uptake_Vmax_Km	0.2	mg biomass day cm-3	Slope for uptake Km-Vmax relationship
Uptake_Vmax_Km_int	0	mg cm-3	Intercept for uptake Km-Vmax relationship
Specif_factor	1		Enzyme efficiency-specificity

120

Supporting Table 2 Substrate concentrations initialized in DEMENT simulations (mg cm^{-3}).

Substrate	C	N	P
DeadMic	0	0	0
DeadEnz	0	0	0
Cellulose	146.89	0	0
Hemicellulose	85.855	0	0
Starch	12.21	0	0
Chitin	4.9952	0.83254	0
Lignin	48.51	0.40425	0
Protein1	10.6	2.09704	0
Protein2	10.6	2.09704	0
Protein3	10.6	2.09704	0
OrgP1	12.48	0	0.478469
OrgP2	1.8182	0.79745	0.478469

121
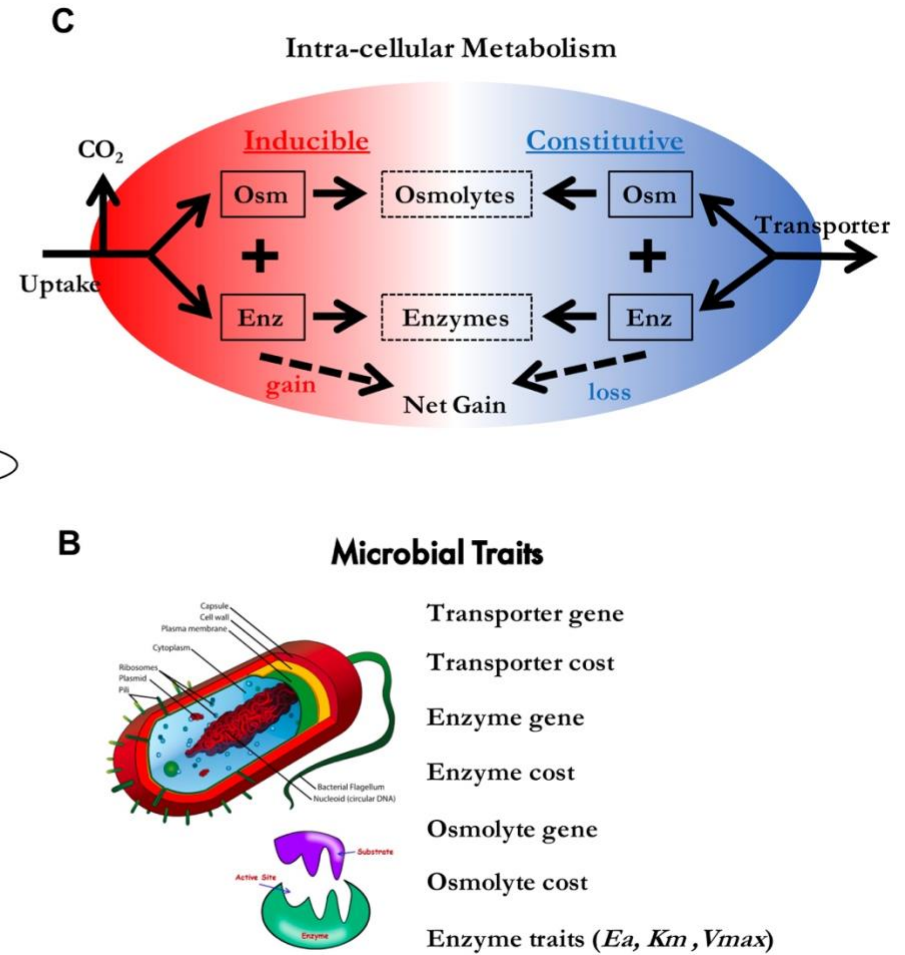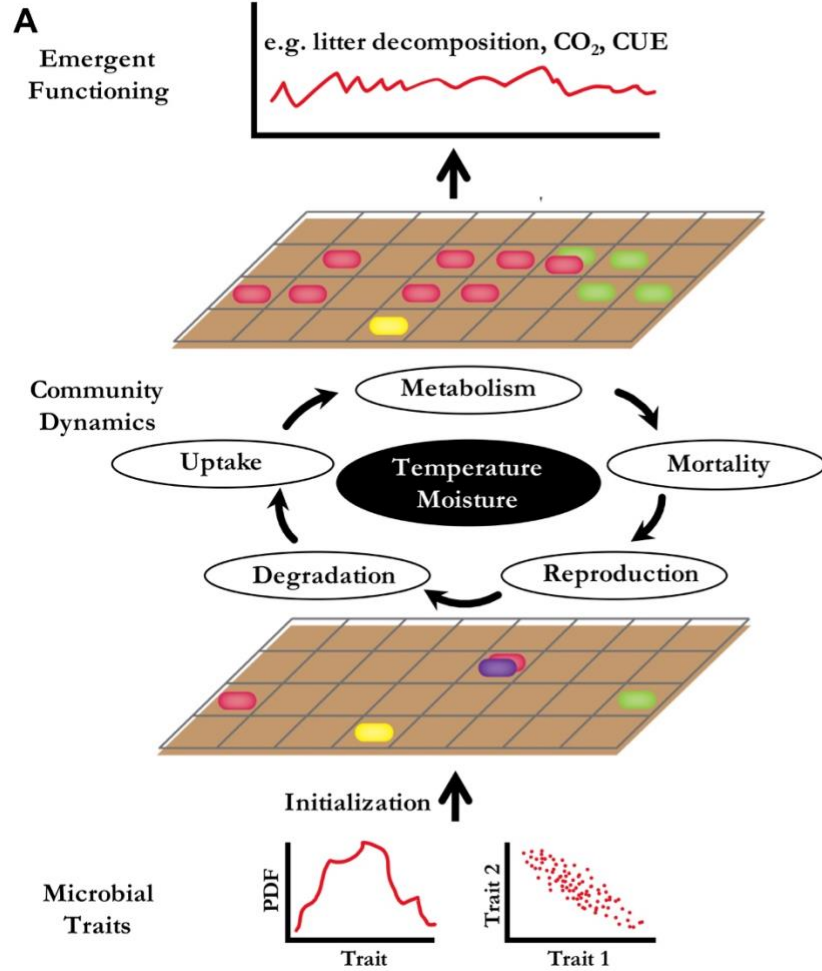
122

123 **Supporting Fig. 1 DEMENTpy conceptual structure (A), microbial traits (B), and intra-cellular metabolism (C).**
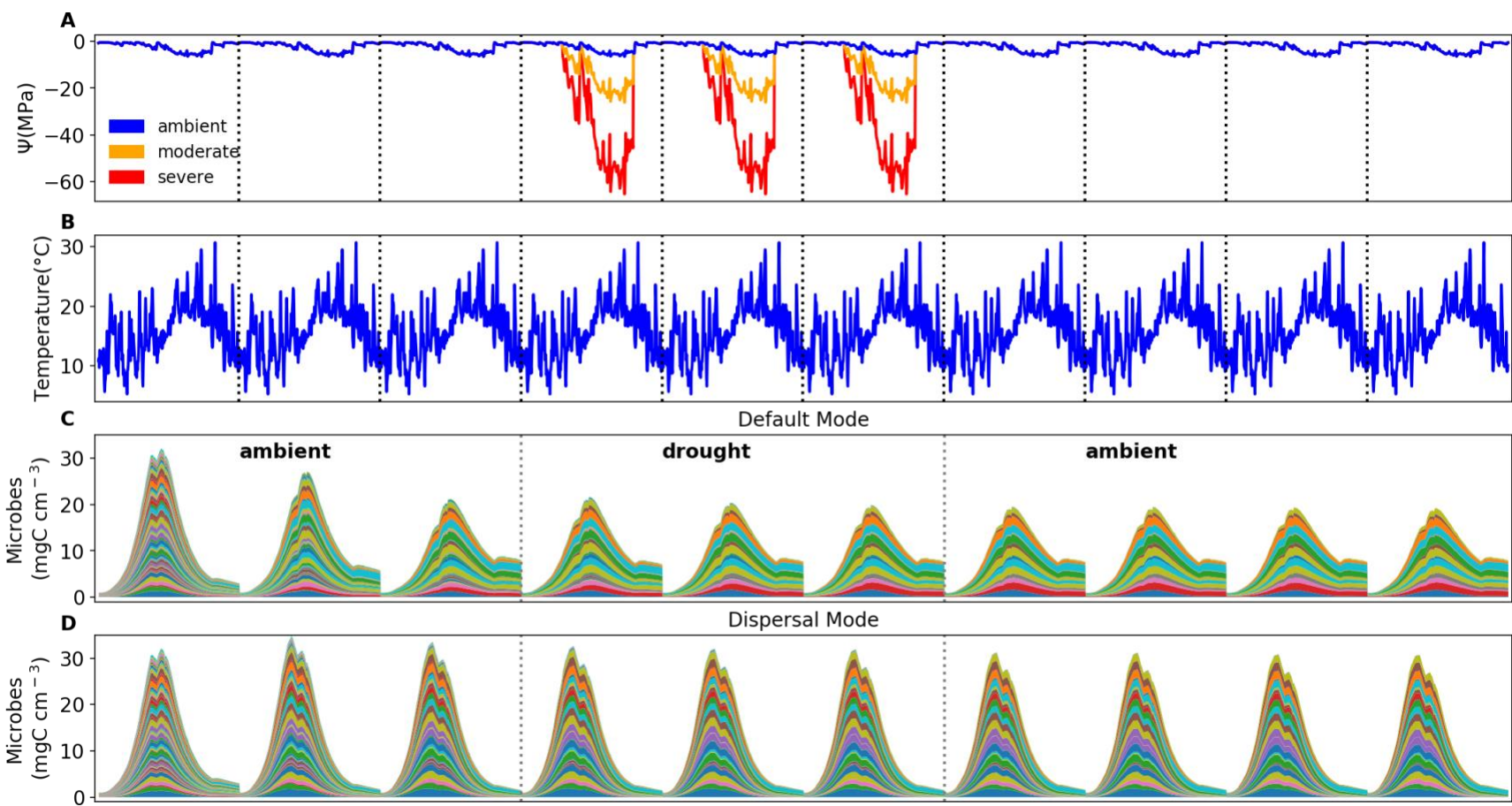
Supporting Fig. 2 Environmental forcing and microbial community dynamics. (**A**) Ambient daily water potential for 2011, with the orange and red lines denoting the moderate and severe drought scenarios, respectively. Drought forcing was obtained by multiplying the ambient water potential across the dry season (from April through September) by 4 and 10, respectively. (**B**) The corresponding daily temperature in 2011. (**C, D**) Microbial community dynamics of the default vs. dispersal mode over 10 years under the ambient

129   scenario. The simulation comprises three phases as separated by the dashed grey lines: a spin-up phase of three years to realize a

130   relatively stable community; a disturbance phase imposing different drought scenarios for three years; and a final recovery phase after

131   drought disturbance for four years. Colored bands represent biomasses of hypothetical taxa.

132
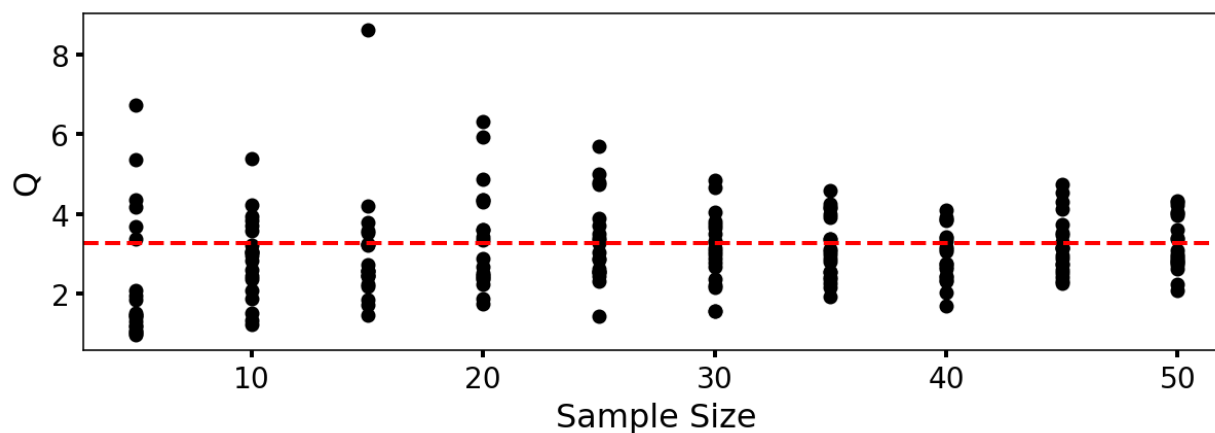
**Supporting Fig. 3 DEMENTpy stochasticity convergence analysis**. Q (quotient) is calculated

as (90% percentile -10% percentile)/median substrate degradation following Bugmann et al.

(1996). Each sample size has 20 replicates that were randomly drawn from a sample pool of 112

runs. This analysis illustrates that a sample size (i.e., ensemble of simulations) of 40 displays

relatively stable, convergent variation that balances the tradeoff between precision and

consumption of computing resources.

139
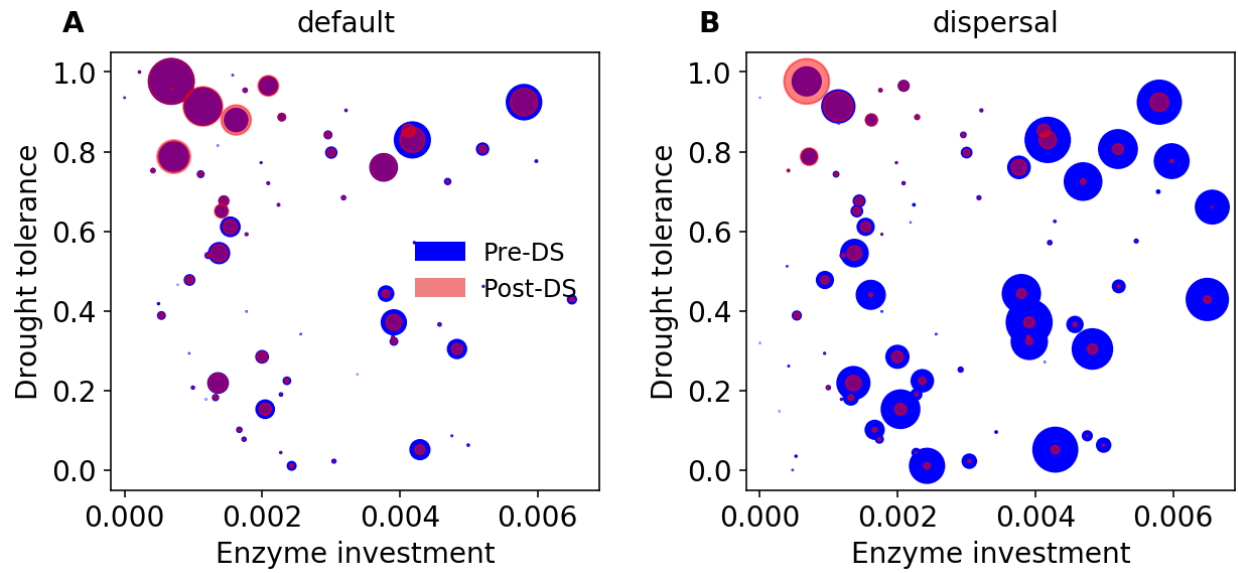
Supporting Fig. 4 Taxonomic changes in traits across the dry season. (A) Taxon-specific traits

of drought tolerance and enzyme investment of a microbial community without dispersal before

(blue) and after the dry season (red) under the ambient scenario. (**B**) The same for a microbial

community with dispersal. Each point corresponds to a different taxon, and the size is proportional

to its biomass.
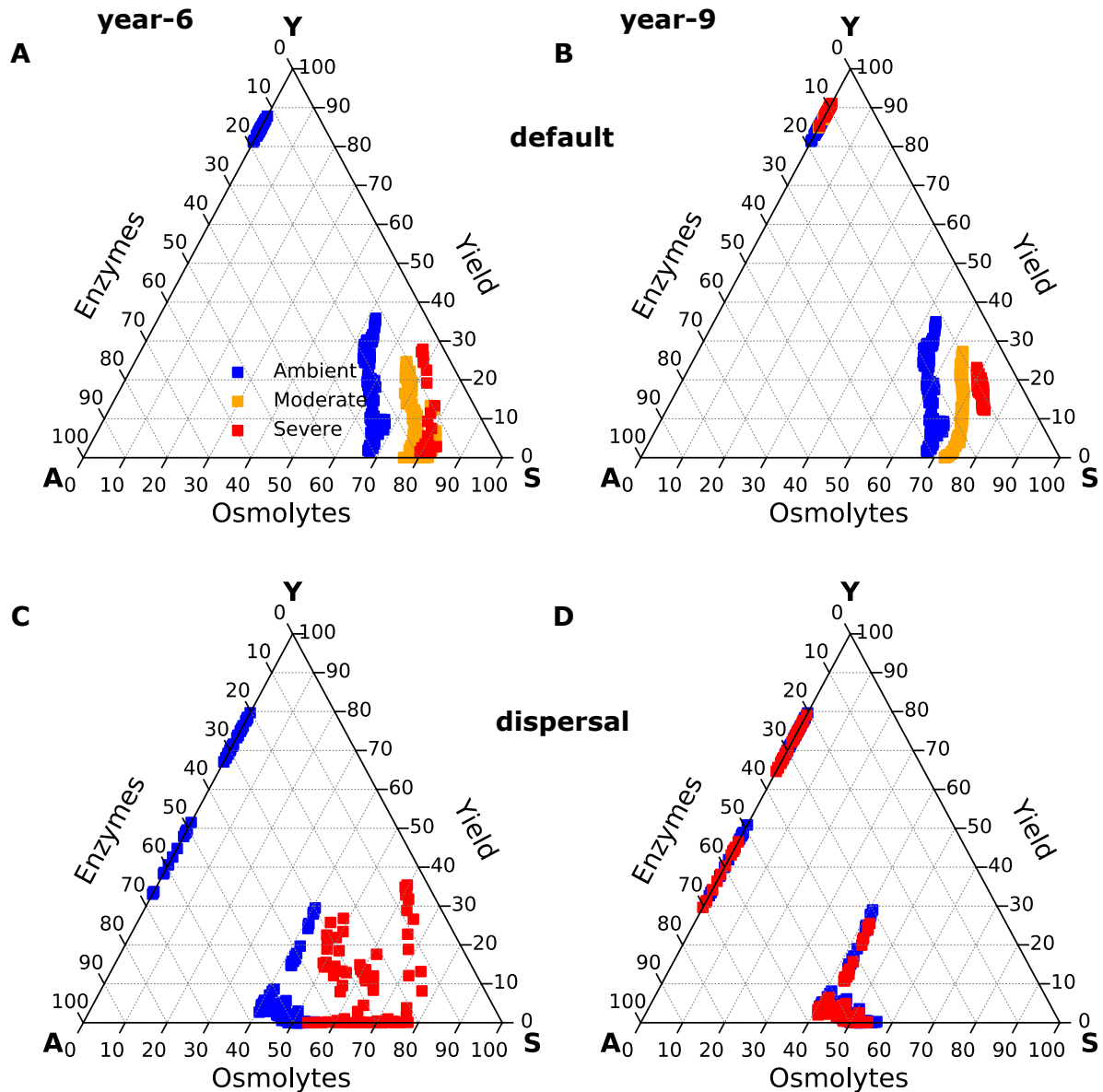
Supporting Fig. 5 Ternary plots of community-level allocation of assimilated carbon among enzymes, osmolytes, and yield over time under different drought scenarios. (A, B) Enzyme-Osmolyte-Yield tradeoff of communities during year 6 (3rd year under drought) and year 9 (3rd year after drought), respectively, of the default mode (without dispersal). (**C, D**) The same for the dispersal mode. The Y (Yield), A (Acquisition), and S (Stress tolerance) labels at the vertices

151 correspond to yield, enzymes, and osmolytes, respectively. Points with negative net biomass gain

152 were omitted.

153
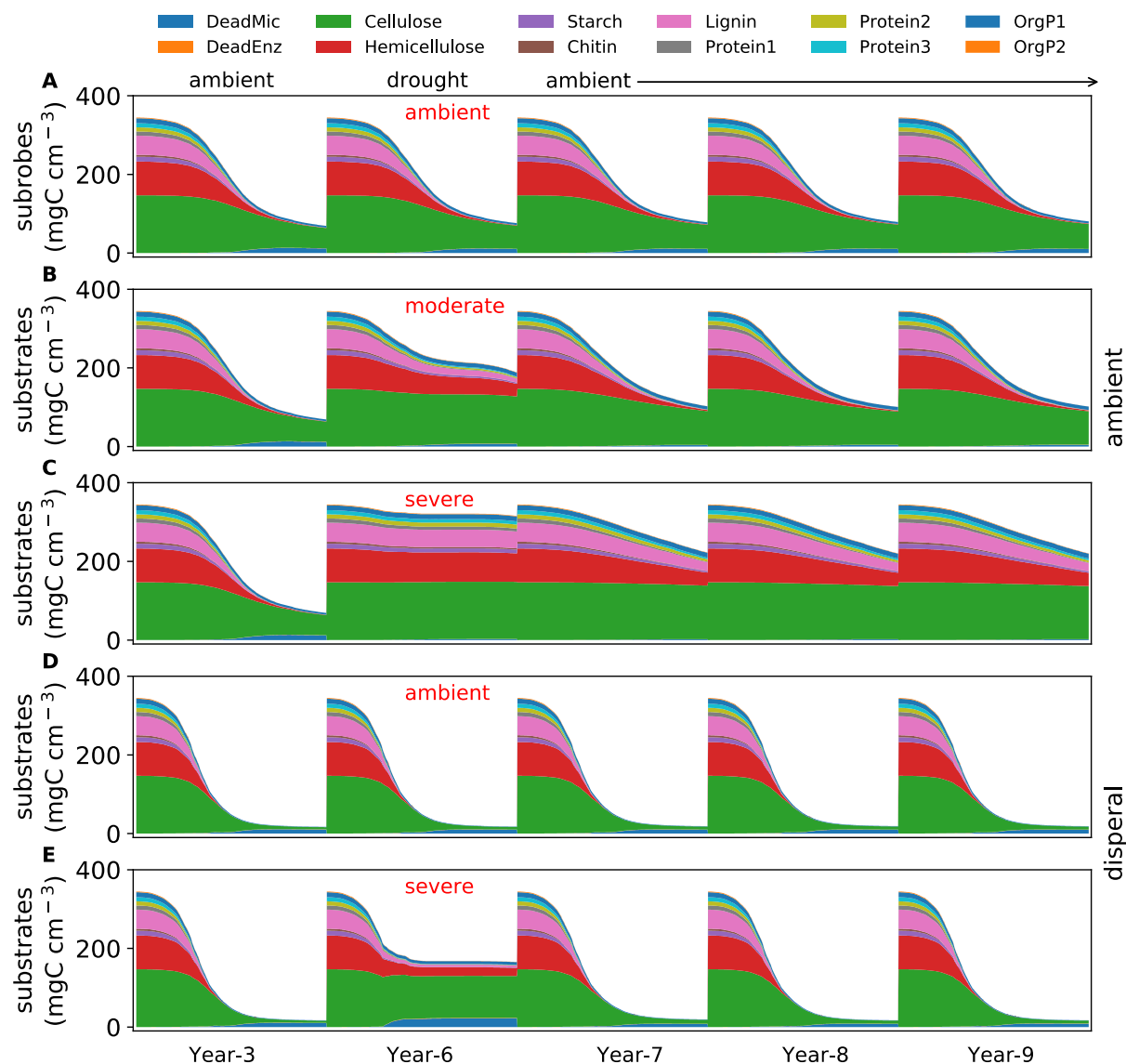
Supporting Fig. 6 Substrate-specific dynamics under differing drought scenarios. (A, B, C) Dynamics under ambient, moderate, and severe drought scenarios in default mode for year 3 and year 6 (the 3rd year under drought disturbance) through year 9. (**D, E**) The same for the dispersal mode but with only ambient and severe scenarios. Each color band represents one type of 12 different substrates.

DEMENTpy Programming Structure

160
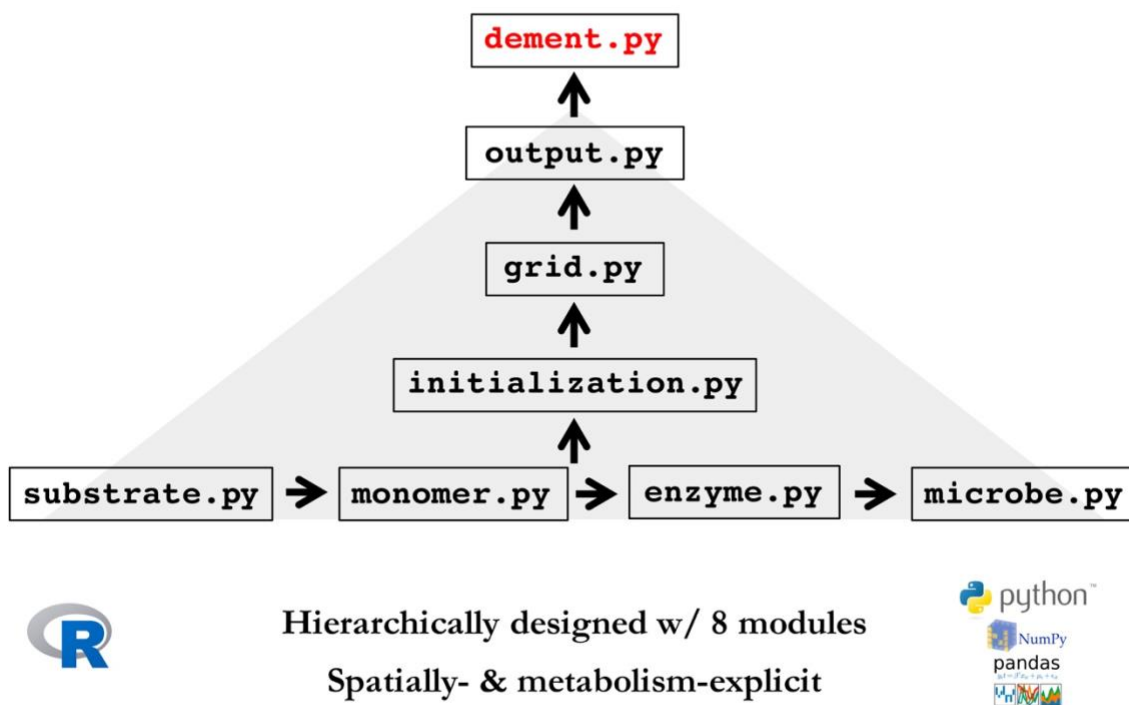
Supporting Fig. 7 DEMENTpy programming structure. DEMENTpy emerges from hierarchically restructuring and mechanistically updating DEMENT, which was programmed in R.